Experimental evidence of various routes of transition from amplitude to oscillation death in coupled oscillators

A.I. Egunjobi[1], Sourav K. Bhowmick[2], O.I. Olusola[3], A.N. Njah[3], and S.K. Dana[4]

[1] Federal University of Agriculture, Abeokuta, Nigeria
(E-mail: `kikelomoteslimot2012@gmail.com`)
[2] Department of Electronics, Asutosh College, Kolkata 700026, India
(E-mail: `souravb1980@gmail.com`)
[3] Department of Physics, University of Lagos, Akoka, Lagos, Nigeria
[4] Department of Physics, University of Lagos, Akoka, Lagos, Nigeria
[5] CSIR-Indian Institute of Chemical Biology, 4, Raja S.C. Mullick Road, Kolkata 700032, India

Abstract. This paper reports experimental evidence of transitions from amplitude death (AD) to oscillation death (OD) in nonlinear oscillator circuits. We use two coupling schemes, basically, a diffusive coupling with repulsive link and another cyclic coupling when we observe three different routes, pitchfork bifurcation, saddle-node bifurcation and transcritical bifurcation as symmetry breaking processes leading to the transition from AD to OD. We use two model systems, the van der Pol oscillator and a Sprott system to design their analog circuits and mainly to observe, in experiment, the theoretical results presented earlier in Phys. Rev. E 89, 032901 (2014).

1 Introduction

Quenching of oscillation in coupled oscillators [1–7] received renewed interest, recently, after the discovery of a Turing type transition [8–13] from amplitude death (AD) to oscillation death (OD). AD denotes a suppression of oscillation to a homogeneous steady state (HSS) which is preferably linked to stabilization of the uncoupled system's equilibrium via Hopf bifurcation. On the other hand, AD to OD transition results in symmetry breaking of the HSS via a pitchfork bifurcation whereby the HSS splits into two stable branches which is defined as inhomogeneous steady states (IHSS) [9]. Such symmetry breaking can also emerge [11] via saddle-node and transcritical bifurcations that depend upon the system dynamics and the form of the coupling. Basically all these symmetry breaking bifurcations during the transition from HSS to IHSS belong to a class of Turing bifurcation.

Studies of quenching in coupled dynamical systems have important practical consequences. The HSS is manifested as stabilization or suppression of oscillation in neuronal system [14]; it is also a desirable goal for control of instabilities in various physical systems such as lasers [15], and its robustness is an important criterion for realization of a desired stable ground state in a healthy cell signalling network [16]. The IHSS has found useful applications in biological systems, such as cell differentiation [17,18], diversity of stable states in coupled genetic oscillators [19], and survival of species [20] etc. In fact, HSS and IHSS may coexist in a multicellular population [18].

In this current study, we report an implementation of electronic oscillators to verify various transition routes (pitchfork, saddle-node, transcritical bifurcations) from AD to OD as mentioned above, in two mutually coupled oscillators with additional repulsive link [10] and cyclic coupling [21] as an experimental evidence of theoretical results reported earlier [11]. Experimental transition from AD (HSS) to OD (IHSS) has been shown using the limit cycle van der Pol (VDP) oscillator and a chaotic Sprott oscillator [23]. This presentation has been structured as follows: two mutually coupled identical VDP oscillators under additional repulsive coupling has been disussed in section II, followed by an example of two mismatched VDP oscillators under cyclic coupling in section III. In section IV, we presented two examples of Sprott oscillators. In one example we used two identical Sprott oscillators under diffusive coupling with additional repulsive link. In the second example, we used two mismatched Sprott oscillators under cyclic coupling. For each example system, we presented experimental evidence of the AD to OD transtion visa-a-vis numerical verification. Additionally we use Xpp-Auto software to identify the type of symmetry breaking process for each example.

2   van der Pol Oscillators: Repulsive coupling

We consider two identical VDP oscillators using mutually diffusive and a repulsive coupling link,

$$
\begin{aligned}
\dot{x}_1 &= y_1 - \epsilon_2(x_1 + x_2) \\
\dot{y}_1 &= \rho(1 - x_1^2)y_1 - x_1 + \epsilon_1(y_2 - y_1) \\
\dot{x}_2 &= y_2 \\
\dot{y}_2 &= \rho(1 - x_2^2)y_2 - x_2 + \epsilon_1(y_1 - y_2)
\end{aligned}
\tag{1}
$$

where $\rho = 0.3$ and ϵ_1 and ϵ_2 are the strengths of mutual diffusive coupling and repulsive coupling links, respectively. After coupling, the system has a fixed point at the origin $(0, 0, 0, 0)$ and the other two fixed points are $(x_1^*, y_1^*, \epsilon_1 y_1^*, 0)$ where $y_1^* = \frac{\epsilon_2 x_1}{1 - \epsilon_1 \epsilon_2}$ and $x_1^* = \pm\sqrt{1 - \frac{1}{\rho \epsilon_2}}$. The repulsive link added to the first equation of (1) that plays a role in a symmetry breaking leading to AD to OD transition. We choose $\epsilon_1 = \epsilon_2 = \epsilon$ for simplicity. Figure $1(a)$ shows a transition first from limit cycle (LC) to AD as the coupling strength increases from $\epsilon > 0$ to $\epsilon = 2$. For further increase beyond $\epsilon = 2$, the coupled system transits from AD to OD.
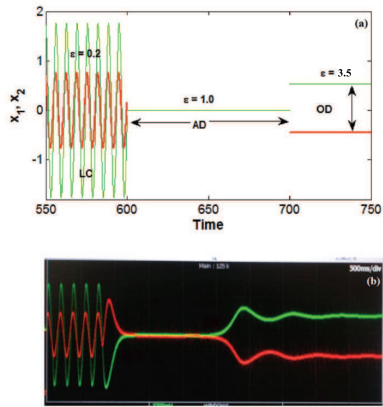
Fig. 1. (Colour online). Transition from AD to OD via pitchfork bifurcation in VDP oscillators under repulsive coupling. (a) Numerical time series of x_1 and x_2, (b) oscilloscope display of experimental time series. The green line indicates x_1 while red line indicates x_2.

The electronic circuit implementation of the coupled VDP is done using microcontroller based programming. The hexadecimal form of the system code is saved in the AVR microcontroller (ATMEGA 328P-PU) EPROM memory using microcontroller programmer. The generated pulse width modulated (PWM) output is fed into a low pass filter to get continuous output waveform to observe in a digital oscilloscope (Yokogawa DL9140, 5GS/s, 1GHz). The frequency of the PWM output may be changed to make it compatible with the bandwidth of the oscilloscope. The timer of the microcontroller is used to change the frequency.
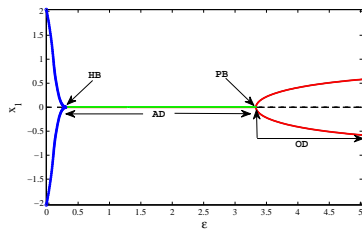
Fig. 2. (Colour online) Extrema of x_1 plotted as functions of coupling strength ϵ for diffusive with repulsive coupled VDP oscillators. The bifurcation diagram shows a transition from oscillatory state (blue colour) to AD (green colour) via Hopf bifurcation and transit to OD (red colour) via Pitchfork bifurcation. Xpp-Auto software is used [24].

Both the numerical and experimental time series are shown for three different coupling strengths as noted in Fig. 1. For $\epsilon = 0.2$, the coupled system depicts a periodic behaviour, then, as the coupling strength is changed to $\epsilon = 1.0$,

it enters the AD state. Finally, for $\epsilon = 3.5$, the coupled system transits to two different steady states, namely, the OD states. A bifurcation plot in Fig. 2 complements the experimental results by confirming the transition from oscillatory behavior to AD via a Hopf bifurcation (HB) at $\epsilon = 0.32$. On the right side, the symmetry breaking transition from AD to OD is shown to emerge via pitchfork bifurcation (PB) at $\epsilon = 3.4$. The blue line on the left side indicates limit cycle oscillation. Remarkably, there is good agreement in numerical and experimental results.

3   VDP Oscillators: Cyclic coupling

We present a second example of coupled VDP oscillators with parameter mismatch and under cyclic coupling. This is a kind of mutual coupling, as if two individuals are interacting with each other via pulling-by-hands and pushing-by-leg and, thereby eastablishing forward and backward push-pull interaction in cyclic order. In the engineering perspective, under the cyclic coupling, one oscillator sends a signal via one pair of variables to the other oscillator while it receives a feedback via another pair of variables [22]. In biological systems, this is similar to neuronal interactions where one neuron sends a signal via one pair of synaptic dendrites and receives a feedback via another pair [25]. The coupled VDP oscillators under cyclic coupling are represented by

$$
\begin{aligned}
\dot{x}_1 &= by_1 \\
\dot{y}_1 &= \rho(1 - x_1^2)y_1 - b_1 x_1 + \epsilon_1(y_2 - y_1) \\
\dot{x}_2 &= y_2 + \epsilon_2(x_1 - x_2) \\
\dot{y}_2 &= \rho(1 - x_2^2)y_2 - b_2 x_2
\end{aligned}
\tag{2}
$$

where $\epsilon_{1,2}$ are the coupling strengths, $\rho = 0.3$ and $b_1 = -1$ and $b_2 = 1$; $\Delta b = b_2 - b_1$ is the parameter mismatch. Altrnatively, the cyclic coupling may be considered by reversing the coupling direction without any affect on the final result. The coupled system has a trivial fixed point at the origin and the other fixed points are $x_1 = \pm\sqrt{1 - \frac{b2 + b\epsilon_1\epsilon_2}{\rho\epsilon_1}}, y_1 = \frac{bx_1}{\rho(1 - x_1^2)}, x_2^* = \epsilon_2 y_1^*$ and $y_2^* = 0$. Figures $3(a)$ and $3(b)$ show the results obtained for cyclic coupling in two VDP oscillators with a parameter mismatch. The system transits from LC to AD at $\epsilon = 0.2$ and then to OD at $\epsilon = 0.90$. The bifurcation points displayed in Fig. 4 show that AD appears via HB and OD via ptichfork bifuraction once again. It is noted that with cyclic coupling, transitions occur at lower coupling compared to conventional mutual coupling.

4   Coupled Sprott oscillators

For demonstration of saddle-node type and transcritical bifurcations during the symmetry breaking process of AD to OD transition, we consider the Sprott system with two different coupling schemes, repulsive links and the cyclic coupling. When we couple two Sprott systems with diffusive coupling and additional repulsive links, the coupled system appears as,
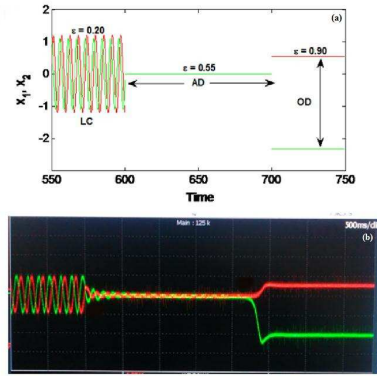
Fig. 3. (Colour online). Transition from AD to OD via pitchfork bifurcation in VDP oscillators under cyclic coupling. (a) Numerical time series. The green line indicates x_1 time series while red indicates x_2 time series. LC exists for $\epsilon = 0.2$, transits to AD for $\epsilon = 0.55$ and to OD for $\epsilon = 0.9$. (b) Oscilloscope pictures of time series.
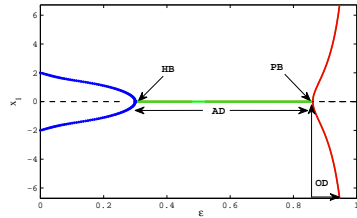
Fig. 4. (Colour online) Extrema of $x_{1,2}$ plotted as functions of coupling strength ϵ for cyclic coupling in VDP oscillators. The bifurcation diagram shows a transition from LC state (blue colour) to AD (green colour) via Hopf bifurcation and to OD (red colour) via pitchfork bifurcation. Xpp-Auto software is used [24].

$$\dot{x_1} = y_1 z_1 + \epsilon_1(x_2 - x_1)$$
$$\dot{y_1} = x_1 + r y_1$$
$$\dot{z_1} = \rho - x_1 y_1$$

$$\dot{x_2} = y_2 z_2 + \epsilon_1(x_1 - x_2)$$
$$\dot{y_2} = x_2 + r y_2$$
$$\dot{z_2} = \rho - x_2 y_2 - \epsilon_2(z_1 + z_2) \qquad (3)$$

where $r = \rho = 1$ for chaotic oscillation, $\epsilon_{1,2}$ represent the coupling strength. The coupled system has fixed points, $x_1^* = r y_1^*$, $y_1^* = \pm \frac{\frac{\rho}{r} - \epsilon_1 \epsilon_2 \pm \sqrt{(\frac{\rho}{r} - \epsilon_1 \epsilon_2)^2 - \frac{4\rho}{r} \epsilon_1 \epsilon_2}}{2\sqrt{\frac{\rho}{r}}}$, $z_1^* = \frac{\epsilon_1(y_1^* - y_2^*)}{x_2^*}$, $x_2^* = \sqrt{r\rho}$, $y_2^* = \pm\sqrt{\frac{\rho}{r}}$ and $z_2^* = \frac{\epsilon_1(y_2^* - y_1^*)}{y_2^*}$. Considering $\epsilon_1 = \epsilon_2 = \epsilon$, we display in Figs. 5($a$) and 5($b$) the numerical simulation and

experimental results respectively. By increasing the coupling strength ϵ, the system dynamics transits from chaotic to periodic behavior via reverse period-doubling and then to AD, and finally to OD state. AD is obtained at $\epsilon \geq 0.40$ while transition to OD occur at $\epsilon \geq 2.40$. We present in Fig. 6 the extrema of $x_{1,2}$ plotted against the coupling strength. The cloudy brown region on the left side shows chaotic behavior of the system at $\epsilon = 0.40$; this is followed by a periodic dynamics for $0.40 < \epsilon \leq 0.48$. Transition to AD occurs via Hopf bifurcation at $\epsilon = 0.48$ as indicated by green colour; further increase of ϵ leads to OD which occurs through saddle-node bifurcation (SNB) at $\epsilon \geq 2.40$. This numerical bifurcation diagram complements the symmetry breaking scenario in Fig. 6.

Finally, we implement the cyclic coupling in chaotic Sprott systems to reveal the transcritical bifurcation during the symmetry breaking process of AD to OD transition. The coupled system under cyclic coupling is,

$$
\begin{aligned}
\dot{x}_1 &= x_1 y_1 - b_1 z_1 + \epsilon_1 (x_2 - x_1) \\
\dot{y}_1 &= x_1 - y_1 \\
\dot{z}_1 &= b x_1 + a z_1
\end{aligned}
\tag{4}
$$

$$
\begin{aligned}
\dot{x}_2 &= x_2 y_2 - b_2 z_2 \\
\dot{y}_2 &= x_2 - y_2 \\
\dot{z}_2 &= x_2 + a z_2 + \epsilon_2 (z_1 - z_2)
\end{aligned}
\tag{5}
$$

$\epsilon_1 = \epsilon_2 = \epsilon$ is the coupling strength, $a = 0.3$ and $b_1 = -1$ and $b_2 = 1$. So we introduce a parameter mismatch in the coupled system. Time series plots of numerical and experimental results are presented in Figs. 7(a) and 7(b). Figures show existence of quasiperiodic and periodic oscillation at $\epsilon \leq 0.29$. The coupled oscillators then transit to AD (HSS) at $\epsilon > 0.29$, and further increase of ϵ leads the system to OD or IHSS at $\epsilon \geq 0.86$. On the left side of the bifurcation diagram in Fig. 8, at $\epsilon < 0.29$, unstable LC oscillation (blue lines) and stable oscillation (red lines are seen followed by quaisperiodic oscillation that transits to periodic oscillation first and then to AD. The system transits to AD at $\epsilon > 0.29$ via HB. OD appears on the right side of the Fig. 8 at $\epsilon \geq 0.86$ via transcritical bifurcation (TB). Results of numerical simulation are in good agreement with experiment.

5   Conclusion

It was shown earlier that the Turing type symmetry breaking process can emerge in two coupled oscillators when the coupled systems transits from HSS to IHSS. It was also shown that three different kinds of bifurcations lead to such a symmetry breaking process, namely, pitchfork bfiurcation, saddle-node bifurcation and transcritical bifurcation; they all belong to Turing type bifurcation. However, such various routes to IHSS state from a HSS emerge under different coupling configuration and it is also system dependent. In this work, we
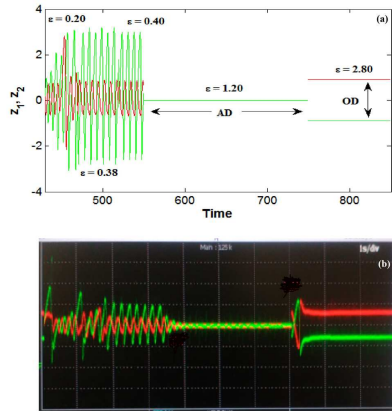
Fig. 5. (Colour online): (a) Numerical time series and (b) real time oscilloscope trace of two coupled Sprott systems under diffusive and additional respulsive links. The red line indicates output from z_1 while green indicates output from z_2
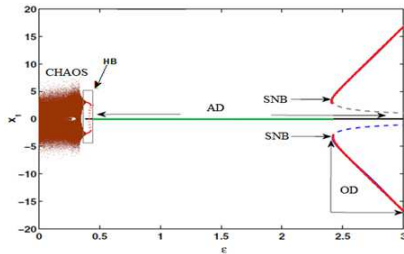
Fig. 6. (Colour online): Bifurcation diagram of $x_{1,2}$ with coupling in Sprott systems under diffusive coupling and one repulsive link. Extrema of $x_{1,2}$ plotted as a function of coupling strength ϵ. It shows a transition from chaotic state (brown colour) to AD (green colour) via Hopf bifurcation (HB) and then to OD (red colour) via saddle-node bifurcation (SNB). Xpp-Auto software is used [24].

presented experimental evidence of all such transitions from HSS to IHSS via various symmetry breaking bifurcations. We took two identical VDP systems under additional repulsive coupling over and above purely diffusive coupling when we found pitchfork bifurcation that led to the transition from AD to OD. We found a similar bifurcation scenario in two mismatched VDP systems under cyclic coupling. Next we considered two Sprott systems first with repulsive coupling, when we found saddle-node bifurcation leading to an AD to OD transition. On the other hand, in two mismatched Sprott systems under cyclic coupling, a transcritical bifurcation led to such a transition. Although these symmetry breaking scenarios were all known from a previous study, however, they were restricted to theoretical studies. We evidence all of them in electronic experiments, for the first time, to the best of our knowledge. We use mainly microcontroller based analog circuit imeplementation and display the results in digital oscilloscope. Worth mentioning that all the numerical bifurcation diagrams were plotted using Xpp-Auto software [24].
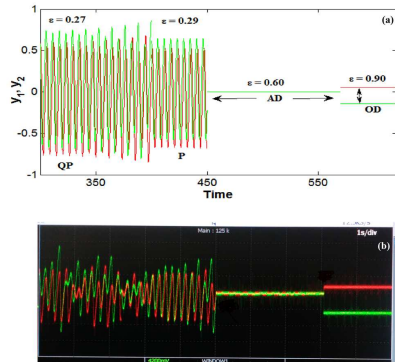
Fig. 7. (Colour online): (a) Numerical time series, and (b) real time oscilloscope trace from cyclically coupled Sprott system. The green outline indicates output from y_1 while red indicates output from y_2.
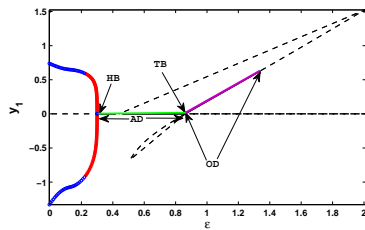
Fig. 8. (Colour online): Extrema of y_1 plotted as functions of coupling strength ϵ for cyclically coupled Sprott oscillators. The bifurcation diagram shows a transition from oscillatory state (blue colour indicates unstable oscillation and red indicates stable oscillation) to AD (green colour) via Hopf bifurcation (HB) and transition to OD (purple colour) via transcritical bifurcation (TB). Xpp-Auto software is used [24].

Acknowledgements

References

1. Garima Saxena, Awadhesh Prasad, Ram Ramaswamy, Amplitude death: The emergence of stationarity in coupled nonlinear systems, Phys. Rep. 521 (5), 205-230 (2012)
2. B. Ermentrout, N. Kopell, Oscillator death in systems of coupled neural oscillators, *SIAM J. Appl. Math.* **50** (1990) 125146.
3. Renato E. Mirollo, Steven H. Strogatz, Journal of statistical physics, July 1990, volume 60, issue 1, pp 245-262.
4. D. V. Ramana Reddy, A. Sen, and G. L. Johnston. Time delayed induced death in coupled limit cycle oscillators. *Phys. Rev. Lett.* **80**, 5109 (1998).

5. K. Konishi. Amplitude death induced by dynamic coupling. *Phys. Rev. E* **68**, 067202 (2003).
6. R. Karnatak, R. Ramaswamy, and A. Prasad. Amplitude death in the absence of time delays in identical coupled oscillators. *Phys. Rev. E* **76**, 035201(R) (2007).
7. V. Resmi, G. Ambika, and R. E. Amritkar. Transitions among the diverse oscillation quenching states induced by the interplay of direct and indirect coupling, *Phys. Rev. E* **84**, 046212 (2011); V. Resmi,G. Ambika, R.E. Amritkar,G. Rangarajan, Amplitude death in complex networks induced by environment. *Phys. Rev. E* **85**, 046211 (2012)..
8. Aneta Koseska, Evgeny Volkov, Jrgen Kurthsa, Oscillation quenching mechanisms: Amplitude vs. oscillation death, Phys. Rep. 531 (4), 173199 (2013).
9. Aneta Koseska, Evgenii Volkov, and Jurgen Kurths. Transition from amplitude to oscillation Death via turing bifurcation. *Phys.Rev.Lett.* **111**, 024103, (2013).
10. C. R. Hens, O. I. Olusola, P. Pal, and S. K. Dana. Oscillation death in diffusively coupled oscillators by local repulsive link. Phys. Rev. E 88, 034902 (2013).
11. C.R. Hens, P. Pal, S.K. Bhowmick, P.K. Roy, A. Sen, S.K. Dana, Diverse routes of transition from amplitude to oscillation death in coupled oscillators under additional repulsive links, *Phys. Rev. E* **89** 032901 (2014).
12. M.Nandan, C.R.Hens, P.Pal, S.K.Dana, Transition from amplitude to oscillation death in a network of oscillator, *Chaos* **24**, 043103 (2014).
13. Wei Zou, D. V. Senthilkumar, Aneta Koseska, and Jrgen Kurths, Generalizing the transition from amplitude to oscillation death in coupled oscillators, *Phys. Rev. E* 88, 050901(R) (2013).
14. G. B. Ermentrout and N. Kopell, Oscillator Death in Systems of Coupled Neural Oscillators, *SIAM J. Appl. Math.* 50(1), 125146 (1990)
15. M.-D. Wei and J.-C. Lun. Amplitude death in coupled chaotic solid-state lasers with cavity-configuration-dependent instabilities. Appl. Phys. Lett. 91, 061121 (2007).
16. D. Kondor and G. Vattay, *PLoS One* **8**, e57653 (2013).
17. N. Suzuki, C. Furusawa, K. Kaneko, Oscillatory protein expression dynamics endows stem cells with robust differentiation potential, *PLoS ONE* **6** (2011) e27232.
18. A. Koseska, E. Ullner, E.I. Volkov, J. Kurths, J.G. Ojalvo, Cooperative differentiation through clustering in multicellular populations, *J. Theor. Biol.* **263** (2010) 189202.
19. E. Ullner, A. Zaikin, E.I. Volkov, J.G. Ojalvo, Multistability and clustering in a population of synthetic genetic oscillators via phase-repulsive cell-to-cell communication, *Phys. Rev. Lett.* **99** (2007) 148103.
20. R. E. Amritkar and Govindan Rangarajan, Spatially Synchronous Extinction of Species under External Forcing, *Phys. Rev. Lett.* 96, 258102 (2006).
21. Bidesh K.Bera, Chittaranjan Hens, Sourav K. Bhowmick, Pinaki Pal, Dibakar Ghosh. Transition from homogeneous to inhomogeneous steady states in oscillators under cyclic coupling. *Physics Letters A* v1.**160**, (2015) P.2 (1-5).
22. O.I. Olusola, A.N. Njah, and S.K. Dana (2013): Synchronization in chaotic oscillators by cyclic Coupling. *European J. of Physics* special topics. **222**, pp 927-937.
23. J.C.Sprott, A new class of chaotic circuit, Phys.Lett. A **228**, 271 (1997).
24. G.B.Ermentrout, Xpp-Auto software, http://www.math.pitt.edu/ bard/xpp/xpp.html.
25. E. Kandel, J. Schwartz, T. Jessell, Principles of Neural Science, McGraw-Hill, USA, 2000.